Title	Characterization of the excess noise conversion from optical relative intensity noise in the photodetection of mode-locked lasers for microwave signal synthesis
Author(s)	Wu, Kan; Shum, Perry Ping; Aditya, Sheel; Ouyang, Chunmei; Wong, Jia Haur; Lam, Huy Quoc; Lee, Kenneth Eng Kian
Citation	Wu, K., Shum, P. P., Aditya, S., Ouyang, C., Wong, J. H., Lam, H. Q., & Lee, K. E. K. (2011). Characterization of the Excess Noise Conversion from Optical Relative Intensity Noise in the Photodetection of Mode-locked Lasers for Microwave Signal Synthesis. Journal of Lightwave Technology, 29(24), 3622-3631.
Date	2011
URL	http://hdl.handle.net/10220/17641
Rights	© 2011 IEEE. Personal use of this material is permitted. Permission from IEEE must be obtained for all other uses, in any current or future media, including reprinting/republishing this material for advertising or promotional purposes, creating new collective works, for resale or redistribution to servers or lists, or reuse of any copyrighted component of this work in other works. The published version is available at: [http://dx.doi.org/10.1109/JLT.2011.2173464].

Characterization of the Excess Noise Conversion from Optical Relative Intensity Noise in the Photodetection of Mode-locked Lasers for Microwave Signal Synthesis

Kan Wu, *Student Member, IEEE,* Perry Ping Shum, *Senior Member, IEEE,* Sheel Aditya, *Senior Member, IEEE,* Chunmei Ouyang, Jia Haur Wong, *Student Member, IEEE,* Huy Quoc Lam and Kenneth Eng Kian Lee, *Member, IEEE*

***Abstract*— Excess noise converted from the optical relative intensity noise (RIN) has limited the noise performance in the microwave signal synthesis application for mode-locked lasers. In this paper, a method for detailed characterization of the excess noise conversion from the optical RIN to the electrical pulse width jitter (PWJ), electrical relative amplitude noise (RAN) and electrical phase noise in the photodetection of mode-locked lasers is proposed. With the measured noise conversion ratios, one can predict the electrical RAN and phase noise power spectral densities under different input optical powers. The effect of the pulse width and peak power of the incident optical pulses and the effect of the saturation power of the photodetectors are also investigated. The results are used to suggest guidelines for achieving low-noise photodetection for microwave signal synthesis application.**

***Index Terms*— Pulse width jitter, intensity noise, phase noise, microwave signal synthesis and mode-locked laser**

I. Introduction

LOW-noise mode-locked lasers have attracted intense interest for various applications including optical sampling [1], low-noise microwave signal synthesis [2] and high-precision clock distribution [3-4]. Many researchers have discussed the noise in the mode-locked lasers [5-10]. Based on their work, various techniques have been proposed to reduce the noise in the mode-locked lasers. These techniques include the use of a slab coupled optical amplifier, cavity filter, optimization of cavity loss, optimization of cavity dispersion and mode locking state, etc. [9-16]. Meanwhile, noise measurement has become more and more accurate [2, 17-19] and the latest optical cross correlation method can provide attosecond accuracy [20-21] and -200 dBc/Hz equivalent phase noise level in the jitter spectrum [15].

For the microwave signal synthesis application, it is well known that photodetectors (PDs) introduce excess noise due to the power dependent pulse broadening and pulse delay [17]. The power dependent pulse broadening leads to the noise conversion from the optical relative intensity noise (RIN) to the electrical pulse width jitter (PWJ) and to the electrical relative amplitude noise (RAN). The power dependent pulse delay leads to the noise conversion from the optical RIN to the electrical phase noise. The RIN-to-phase-noise conversion has been discussed both in time domain and in frequency domain [22-23]. Here, the electrical RAN includes the electrical RAN of the pulse amplitude and the electrical RAN of the signal at repetition frequency f_R. The electrical RAN of the pulse amplitude means the amplitude noise of the pulse peak voltage and the electrical RAN at f_R means the amplitude noise of the component at repetition frequency f_R (the amplitude at f_R can be obtained as the square root of the RF power at f_R). These two RANs are not the same because the electrical PWJ also contributes to the electrical RAN at f_R which is the RAN that can be experimentally measured.

In the above context, many novel designs have been proposed to overcome the excess phase noise and these have demonstrated a residual timing jitter of the extracted RF signals as low as a few femtoseconds [24-25]. However, the RIN-to-PWJ (here and subsequent mentions of PWJ refer to the PWJ of the electrical pulses) and RIN-to-RAN (including the electrical RAN of the pulse amplitude and the electrical RAN of the signal at repetition frequency f_R, or RAN at f_R for short) conversion are not fully understood yet. Also, the relation between the electrical RAN of the pulse amplitude and the electrical RAN at f_R is unclear. Further, previous work on PWJ measurement of the optical pulses focuses on pulse widths larger than the rise time of the PDs and neglects the excess noise in the PDs [26-28]. Due to the ultralow quantum limited noise of the femtosecond lasers, the mode-locked lasers used in microwave signal synthesis usually have a pulse width much shorter than the rise time of the PDs which means the output of the PD can be regarded as its impulse response. Therefore it is

Manuscript received August 14, 2011.

This work is partially supported by the Defence Research and Technology Office, Ministry of Defence, Singapore.

K. Wu, P. Shum, S. Aditya, C. Ouyang, J. H. Wong and are with the School of Electrical & Electronic Engineering, Nanyang Technological University, Singapore 637553 (e-mail: wuka0002@ ntu.edu.sg; EPShum@ntu.edu.sg).

P. Shum is also with CINTRA CNRS/NTU/THALES, UMI 3288, Research Techno Plaza, 50 Nanyang Drive, Border X Block, Level 6, Singapore 637553

H. Q. Lam and K. E. Lee are with the Temasek Laboratories, Nanyang Technological University, Singapore 637553.

meaningful to develop a method that can completely characterize these kinds of noise conversion from PDs, that is, RIN-to-PWJ, RIN-to-RAN (the electrical RAN of the pulse amplitude), RIN-to-RAN (the electrical RAN at f_R) and RIN-to-phase-noise conversion, for microwave signal synthesis application based on femtosecond mode-locked laser. Also, it is still unclear how the pulse width and peak power of the incident optical pulses affects these 4 kinds of noise conversion. Moreover, we notice that in many applications of femtosecond lasers in microwave signal synthesis, a wideband PD is usually used. This may inherently suggest that a wideband PD should have a low RIN-to-phase-noise. However, our comparison of two PDs with 10 GHz and 2 GHz bandwidth respectively, shows that this is not necessarily true and the saturation power of the PDs may play an even more important role to achieve low RIN-to-phase-noise conversion.

In this paper, we discuss the detailed characterization of RIN-to-PWJ, RIN-to-RAN (including the electrical RAN of the pulse amplitude and the RAN at f_R) and RIN-to-phase-noise conversion in the PDs when detecting the optical pulses from femtosecond mode-locked lasers. The noise conversion ratios are experimentally determined by analyzing the electrical pulse profiles and measuring the power at f_R under different input optical powers. Theoretical analysis which considers the pulse asymmetry and uses the Fourier series analysis, is also performed to describe the relation among all these noise conversion ratios and to enable one to predict the electrical RAN and phase noise power spectral densities (PSDs). The effect of the incident optical pulse width and peak power of the optical pulses and the effect of the saturation power of the PDs are also investigated. Finally, the results of the above studies are used to provide many useful guidelines for low-noise photodetection for microwave signal synthesis application. The discussion in this paper is limited to the condition that the optical pulse width is much smaller than the rise time of the PDs and therefore the output of the PD can be regarded as its impulse response.

The paper is arranged as follows. Section II is the theoretical model of a noisy electrical pulse train. Section III discusses the measurement of the noise conversion ratios experimentally. Section IV investigates the effect of incident optical pulse width and peak power. Section V investigates the effect of saturation power of PDs. Section VI presents the conclusion.

II. THEORETICAL MODEL OF A NOISY ELECTRICAL PULSE TRAIN

A noisy electrical pulse train obtained from photodetection of an optical pulse train can be expressed by

$$V = V_0 \sum_{n=-\infty}^{+\infty} (1+\Delta a_n)\, f\left(\frac{t-nT+\Delta t_n}{\tau+\Delta\tau_n}\right) \tag{1}$$

where V_0 is the pulse amplitude (voltage), $f(t/\tau)$ is the normalized amplitude profile of a single pulse, τ is the pulse width, T is the time period, Δa_n is the electrical RAN of pulse amplitude, Δt_n is the timing jitter and $\Delta\tau_n/\tau$ is the electrical PWJ. Eq.(1) can be simplified using Taylor expansion so that

$$V/V_0 = \left(\sum_{n=-\infty}^{+\infty} f\left(\frac{t-nT}{\tau}\right)\right)(1+\Delta a(t)) + \left(\sum_{n=-\infty}^{+\infty} \dot{f}\left(\frac{t-nT}{\tau}\right)\right)\frac{\Delta t(t)}{\tau} - \left(\sum_{n=-\infty}^{+\infty} \dot{f}\left(\frac{t-nT}{\tau}\right)\frac{t-nT}{\tau}\right)\frac{\Delta\tau(t)}{\tau} \tag{2}$$

where $\Delta t(t)=\Delta t_n$, $(nT-T/2) < t \le (nT+T/2)$, is the continuous expression of Δt_n and the same definition can be applied to $\Delta\tau(t)$ and $\Delta a(t)$, and $\dot{f} = df(x)/dx = \tau df(t/\tau)/dt$ (for simplicity, we use Δt, $\Delta\tau$ and Δa to represent the corresponding time varying quantities in the subsequent expressions). All higher order noise terms have been neglected and only first order noise terms are considered. More details of the derivation of Eq.(2) can be found in the works of von der Linde [6] or L. P. Chen [29]. Since the pulse profile is not symmetric, we need to consider both the even part (defined as f_e) and the odd part (defined as f_o) of the pulse profile f, where $f = f_e + f_o$. The periodicity of the terms in Eq.(2) means that these can be expanded into a Fourier series as follows:

$$\sum_{n=-\infty}^{+\infty} f_e\left(\frac{t-nT}{\tau}\right) = \frac{a_0}{2} + \sum_{k=1}^{+\infty} a_k \cos k\omega_R t \tag{3}$$

$$\sum_{n=-\infty}^{+\infty} \dot{f}_e\left(\frac{t-nT}{\tau}\right)\frac{1}{\tau} = -\sum_{k=1}^{+\infty} a_k k\omega_R \sin k\omega_R t \tag{4}$$

$$\sum_{n=-\infty}^{+\infty} \dot{f}_e\left(\frac{t-nT}{\tau}\right)\frac{t-nT}{\tau} = -\frac{a_0}{2} + \sum_{k=1}^{+\infty} (c_k - a_k)\cos k\omega_R t \tag{5}$$

$$\sum_{n=-\infty}^{+\infty} f_o\left(\frac{t-nT}{\tau}\right) = \sum_{k=1}^{+\infty} b_k \sin k\omega_R t \tag{6}$$

$$\sum_{n=-\infty}^{+\infty} \dot{f}_o\left(\frac{t-nT}{\tau}\right)\frac{1}{\tau} = \sum_{k=1}^{+\infty} b_k k\omega_R \cos k\omega_R t \tag{7}$$

$$\sum_{n=-\infty}^{+\infty} \dot{f}_o\left(\frac{t-nT}{\tau}\right)\frac{t-nT}{\tau} = \sum_{k=1}^{+\infty} (d_k - b_k)\sin k\omega_R t \tag{8}$$

where $\omega_R = 2\pi f_R = 2\pi/T$ is the fundamental repetition angular frequency. The definition and calculation of the Fourier coefficients a_k to d_k are given in the Appendix. The final expression of a noisy electrical pulse train can be written as

$$\begin{aligned} V/V_0 &= \frac{a_0}{2}\left(1+\Delta a+\frac{\Delta\tau}{\tau}\right) + \sum_{k=1}^{+\infty} (I_k \cos k\omega_R t - Q_k \sin k\omega_R t) \\ &= \frac{a_0}{2}\left(1+\Delta a+\frac{\Delta\tau}{\tau}\right) + \sum_{k=1}^{+\infty} A_k \cos(k\omega_R t + \varphi_k) \end{aligned} \tag{9}$$

where I_k and Q_k are the amplitudes of two orthogonal frequency components respectively and their expressions are given by

$$I_k = a_k(1+\Delta a) - (c_k - a_k)\frac{\Delta\tau}{\tau} + b_k\omega_R\Delta t \tag{10}$$

$$Q_k = -b_k(1+\Delta a) + (d_k - b_k)\frac{\Delta\tau}{\tau} + a_k k\omega_R\Delta t \tag{11}$$

The total amplitude A_k and phase φ_k can then be calculated as

$$\begin{aligned} A_k &= \sqrt{I_k^2 + Q_k^2} \\ &= \sqrt{(a_k^2 + b_k^2)(1+2\Delta a) + (a_k^2 - a_k c_k + b_k^2 - b_k d_k)\frac{2\Delta\tau}{\tau}} \\ &\approx \sqrt{a_k^2 + b_k^2}\left(1 + \Delta a + \frac{a_k^2 - a_k c_k + b_k^2 - b_k d_k}{a_k^2 + b_k^2}\frac{\Delta\tau}{\tau}\right) \\ &\equiv \sqrt{a_k^2 + b_k^2}\left(1 + \Delta a + C_a\frac{\Delta\tau}{\tau}\right) \end{aligned} \tag{12}$$

$$\begin{aligned} \varphi_k &= \tan^{-1} Q_k / I_k \\ &= \tan^{-1}\frac{-b_k(1+\Delta a) + (d_k - b_k)\frac{\Delta\tau}{\tau} + a_k k\omega_R\Delta t}{a_k(1+\Delta a) - (c_k - a_k)\frac{\Delta\tau}{\tau} + b_k\omega_R\Delta t} \\ &\approx \tan^{-1}\left(-\frac{b_k}{a_k}\right) + k\omega_R\Delta t + \frac{a_k d_k - b_k c_k}{a_k^2 + b_k^2}\frac{\Delta\tau}{\tau} \\ &\equiv \tan^{-1}\left(-\frac{b_k}{a_k}\right) + k\omega_R\Delta t + C_\varphi\frac{\Delta\tau}{\tau} \end{aligned} \tag{13}$$

where the relation $d\tan^{-1}(x)/dx = 1/(1+x^2)$ is used. The two coefficients C_a and C_φ are defined as:

$$C_a = \frac{a_k^2 - a_k c_k + b_k^2 - b_k d_k}{a_k^2 + b_k^2}$$

$$C_\varphi = \frac{a_k d_k - b_k c_k}{a_k^2 + b_k^2}$$

Since A_k (k=1) in Eq.(12) represents the amplitude of the signal at f_R, the noise terms in A_k (k=1) represent the electrical RAN at f_R. As mentioned earlier, Δa is the electrical RAN of the pulse amplitude and $\Delta\tau/\tau$ is the electrical PWJ. Therefore Eq. (12) indicates that

$$RAN_R = RAN_P + C_a \cdot PWJ \tag{14}$$

where RAN_R is the electrical RAN at f_R and RAN_P is the electrical RAN of the pulse amplitude. If we denote the RIN-to-RAN (RAN at f_R) conversion ratio as r_{RAN_R}, RIN-to-RAN (pulse amplitude) conversion ratio as r_{RAN_P} and RIN-to-PWJ conversion ratio as r_{PWJ}, Eq.(14) can be written as

$$r_{RAN\_R} = r_{RAN\_P} + C_a r_{PWJ} \tag{15}$$

The expressions for r_{RAN_R}, r_{RAN_P} and r_{PWJ} are given by

$$r_{RAN\_R} = \frac{dV_R/V_R}{dP/P} = \frac{P}{V_R}\frac{dV_R}{dP} \tag{16}$$

$$r_{RAN\_P} = \frac{dV_P/V_P}{dP/P} = \frac{P}{V_P}\frac{dV_P}{dP} \tag{17}$$

$$r_{PWJ} = \frac{d\tau/\tau}{dP/P} = \frac{P}{\tau}\frac{d\tau}{dP} \tag{18}$$

where V_R is the amplitude at f_R, P is the input optical power, V_P is the electrical pulse amplitude and τ is the electrical pulse width. The values of V_P and τ can be obtained by analyzing the electrical pulse profiles measured using a high-speed oscilloscope and V_R can be obtained as the square root of the RF power at f_R measured by an RF spectrum analyzer. That means the left hand side and the right hand side of Eq.(15) can be obtained independently. Thus one can verify the validity of Eq.(15).

Suppose the PSD of the laser RIN is S_{RIN_laser}. Then the PSD of the electrical RAN at f_R, the PSD of the electrical RAN of pulse amplitude, and the PSD of PWJ are given by

$$S_{RAN\_R} = r_{RAN\_R}^2 S_{RIN\_laser} \tag{19}$$

$$S_{RAN\_P} = r_{RAN\_P}^2 S_{RIN\_laser} \tag{20}$$

$$S_{PWJ} = r_{PWJ}^2 S_{RIN\_laser} \tag{21}$$

In a similar manner, the phase at f_R consists of three parts: 1) a pulse-profile-related term $\tan^{-1}(-b_k/a_k)$ – since the pulse profile is related to the input optical power, this term in fact contains the information about the laser RIN; 2) the original phase noise (or timing jitter) of the laser; and 3) the PWJ induced noise with a coefficient C_φ. It has been shown that the RIN-to-phase-noise conversion ratio r_{PN} can be obtained by Fourier transformation of the electrical impulse response of a PD to extract the phase and then differentiating the phase with respect to the input optical power [22]. Therefore, the expression for r_{PN} (with the units of rad) is given by

$$r_{PN} = \frac{d\varphi}{dP/P} = -P\frac{d\tan^{-1}(b_k/a_k)}{dP} \approx -P\frac{d(b_k/a_k)}{dP} \tag{22}$$

where the timing jitter and the PWJ in Eq.(13) are assumed zero because we use the average phase of the electrical pulses. The measured electrical phase noise PSD is then given by

$$S_\varphi = S_{\varphi\_laser} + (r_{PN} + C_\varphi r_{PWJ})^2 S_{RIN\_laser} \tag{23}$$

For microwave signal synthesis applications, femtosecond mode-locked lasers are generally chosen as the pulse sources due to their ultra-low quantum limited noise. Therefore, we are more interested in the pulses with a duty cycle $\sigma = \tau/T$ less than 1%. Under this condition, the Fourier coefficient a_k is much greater than the remaining three coefficients b_k to d_k at f_R, i.e., k=1, and thus the coefficient $C_a \approx 1$ and $C_\varphi \approx 0$. Eqs.(15) and (23) can thereby be simplified as

$$r_{RAN\_R} = r_{RAN\_P} + r_{PWJ} \tag{24}$$

$$S_\varphi = S_{\varphi\_laser} + r_{PN}^2 S_{RIN\_laser} \tag{25}$$

An example of C_a and C_φ values at f_R calculated from the measured electrical pulse profiles for different input optical powers entering a 10 GHz PD is shown in the inset of Fig.2 in the next section.

III. MEASUREMENT OF RIN-TO-PWJ, RIN-TO-RAN AND RIN-TO-PHASE-NOISE CONVERSION RATIOS

The impulse response method proposed by J. Taylor [22] has been proven to be an effective method to characterize the RIN-to-phase-noise conversion in the PDs. As shown in Fig.1, we use a similar setup to measure the RIN-to-PWJ and RIN-to-RAN (including the electrical RAN of pulse amplitude and the electrical RAN at f_R) conversion in the PDs. A homemade 66.1 MHz mode-locked fiber laser centered at 1566 nm is used as the pulse source generating a pulse train with a spectral width of ~11 nm and an average optical power of 2.5 mW. A variable optical attenuator (VOA) controls the optical power incident on a 10 GHz InGaAs PD (EOT ET3500F). The temporal profile of the electrical pulses after photodetection is measured by a high-speed real-time oscilloscope (LeCroy SDA820Zi-A) with a bandwidth of 20 GHz. The oscilloscope has a real-time sampling rate of 40 Gsamples/s and works under RIS mode which has an equivalent sampling rate of 200 Gsamples/s, corresponding to a time interval of 5 ps. The timing accuracy of the oscilloscope is ~250 fs. The nonlinearity in the amplitude response of the oscilloscope is found to be small by comparing the waveforms obtained with and without a 10 dB electrical attenuator between the PD and the oscilloscope. The RIN and phase noise at the repetition frequency are measured by a signal source analyzer (SSA, R&S FSUP26). A low pass filter (LPF) and low noise amplifier (LNA) are inserted before the SSA in order to extract the frequency component at the repetition frequency and to provide enough input power for SSA noise measurement.

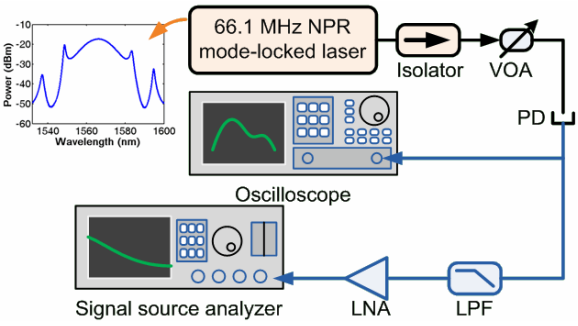

Fig.1. Experimental setup for the measurement of noise conversion in the PD. VOA: variable optical attenuator; PD: photodetector; LPF: low pass filter; LNA: low noise amplifier

A. RIN-to-PWJ and RIN-to-RAN conversion

The measured electrical pulse profiles are shown in Fig.2 as the input optical power varies from 0.1 mW to 2.1 mW. The inset in Fig.2 shows the calculated coefficients C_a and C_φ at f_R, confirming that $C_a \approx 1$ and $C_\varphi \approx 0$ for all values of input power. Fig.3 (a) shows the corresponding electrical pulse width and electrical pulse amplitude values. With these data, the RIN-to-PWJ and the RIN-to-RAN (pulse amplitude) ratios r_{PWJ} and r_{RAN_P} can be calculated according to Eq.(17) and (18), respectively; the results are shown as red and green curves in Fig.3 (b). The derivatives required in Eq.(17) and (18) are calculated using the central difference of the data in Fig.3 (a). The smooth curves for the conversion ratios are obtained by using third-order polynomial fit. The signal amplitude at f_R is measured using an RF spectrum analyzer and the RIN-to-RAN ratio at f_R, r_{RAN_R}, calculated according to Eq.(16), is shown as dashed black curve in Fig.3 (b). It can be seen that the measured values of r_{RAN_R} are very similar to those calculated by summing r_{PWJ} and r_{RAN_P} according to Eq.(24) (blue curve); this confirms the validity of the analysis presented in Section II. The discrepancy in the two sets of values of r_{RAN_R} arises due to two reasons: one is the measurement error of the electrical pulse profiles and the input optical powers because the dP term in the denominator of Eqs.(16)-(18) amplifies the error in P and the P in the numerator amplifies the errors in $d\tau/\tau$ and dV/V when P is large. This explains the relatively larger discrepancy for P > 1.5 mW. The other reason is the bandwidth limitation (~17 GHz) set by the oscilloscope. The inset in Fig.3 (a) shows the envelope of the RF spectra of the electrical signal from the PD at 0.1 mW and 2 mW input powers. It can be seen that for 0.1 mW input power, the RF power levels at 15 GHz ~ 20 GHz are still comparatively high; the suppression of these power levels leads to pulse broadening and thus an underestimation of the PWJ. On the other hand, for 2 mW input power, the RF power levels after 2 GHz decrease quickly. Therefore, the bandwidth limitation effect is stronger when the input power is low. One more example of r_{RAN_R}, r_{RAN_P} and r_{PWJ} calculations is given in Fig.8 in the next section in which the values of the optical powers are recorded with a higher accuracy (1 μW) and a better match between r_{RAN_R} and $r_{RAN\_P}+r_{PWJ}$ is found at high input power range (0.6 mW ~ 2 mW). The discrepancy at input power less than 0.6 mW still exists due to the limitation of the oscilloscope.

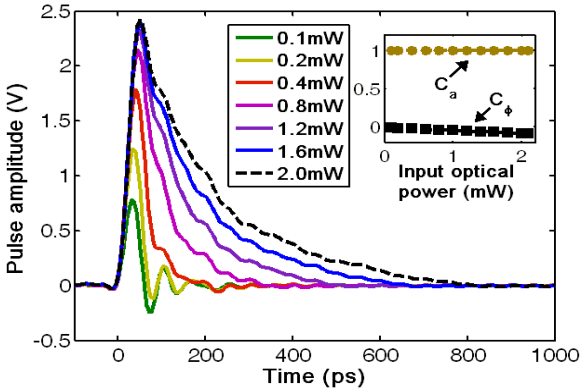

Fig.2. Electrical pulse profiles for different input optical powers entering the 10 GHz PD. Inset: Coefficients C_a and C_φ at repetition frequency f_R for different input optical powers

Since the values of r_{RAN_R} calculated by summing r_{PWJ} and r_{RAN_P} are more sensitive to the measurement error than the one directly obtained from the measurement of the RF power at f_R, we use the latter to estimate the laser RIN PSD from the measured electrical RAN PSDs at f_R at various input optical powers based on Eq.(19). The estimated laser RIN PSD is shown in Fig.4 and the PSD values at 1 kHz and 10 kHz offset frequencies are also plotted for comparison. With the laser RIN PSD known, one can easily calculate the PSD of PWJ and RAN of pulse amplitude using Eqs.(20) and (21). As can be seen, good agreement is obtained between the calculated and measured values.

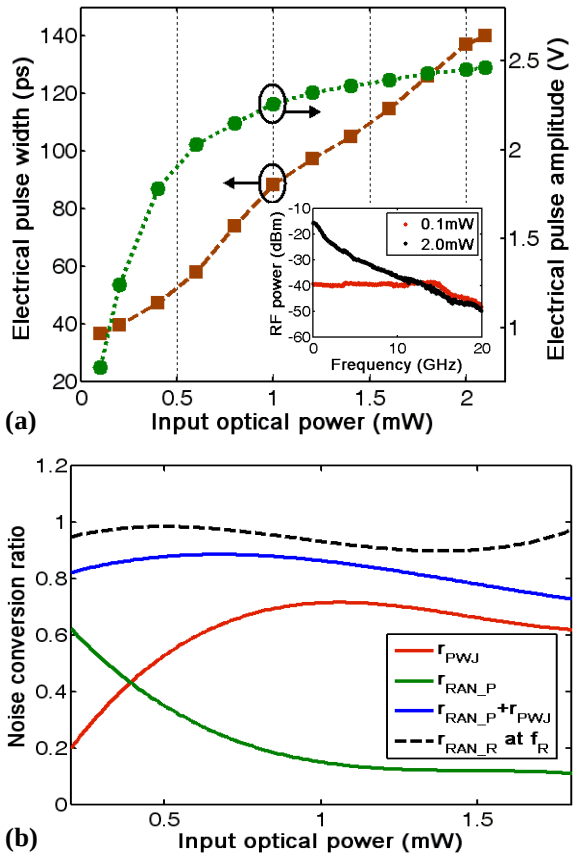

Fig.3. (a) Electrical pulse widths and amplitudes. (b) Noise conversion ratios RIN to PWJ (r_{PWJ}), RIN to RAN of pulse amplitude (r_{RAN_P}) and RIN to RAN at f_R (r_{RAN_R}). Inset in (a) is the envelope of the RF spectra of the electrical signals from the PD at 0.1 mW and 2 mW input power

The output electrical power of the PD is determined by the input optical power and the quantum efficiency (or responsivity) of the PD. This limits the total output power of the PD to a few milli-watts considering a quantum efficiency of 1 and a maximum allowed input power of 10 mW. The power levels at each frequency component are thus even lower. Also, the power levels at lower frequencies increase quickly with the increasing input power whereas the power levels at higher frequencies increase very slow or even decrease due to the PD saturation effect (see inset of Fig.3 (a)). Therefore if one wants to get high output power at a certain frequency one may increase the input optical power at the expense of a higher RIN-to-phase-noise conversion (will be discussed in the next section) and a low-noise post-amplifier may also be required.

B. RIN-to-phase-noise conversion

The RIN-to-phase-noise conversion ratio can be obtained by analyzing the phase values of the electrical pulses measured for different input power levels. The phase values calculated by Eq.(13) (note that the timing jitter and PWJ terms in Eq.(13) are assumed zero because we are considering the average phases) are shown in Fig.5 (a). We calculate the phase values for frequencies ranging from the repetition frequency f_R = 66.1 MHz to the 151th harmonic 151f_R = 9.98 GHz. Then we use a fourth-order polynomial to fit the phase values and calculate the corresponding RIN-to-phase-noise conversion ratios r_{PN} (absolute values) based on Eq.(22); these results are shown in Fig.5 (b). Fig.5 (c) gives three examples of the RIN-to-phase- noise conversion ratios at 66.1 MHz, 1983 MHz and 9981.1 MHz, respectively, which correspond to the three dashed lines in Fig.5 (b). These ratios are exactly the same as the ones calculated by the method of direct Fourier transformation of the pulse profiles used in Ref. [22].

Knowing the RIN-to-phase-noise conversion ratio r_{PN}, we can predict the measured phase noise PSD according to Eq.(25). The laser phase noise PSD is the PSD measured at low input power where the value of r_{PN} is very small and therefore the noise term converted from the laser RIN is negligible. Fig.6 (a) shows an example of phase noise PSD prediction at an input power of 1.4 mW. The ratio r_{PN} is 0.051, corresponding to a decrease of laser RIN PSD of ~25.8 dB. Fig.6 (b) shows the predicted and measured phase noise PSD values at 1 kHz and 10 kHz offset frequencies under different input powers. It can be seen that the predicted and measured values match well.

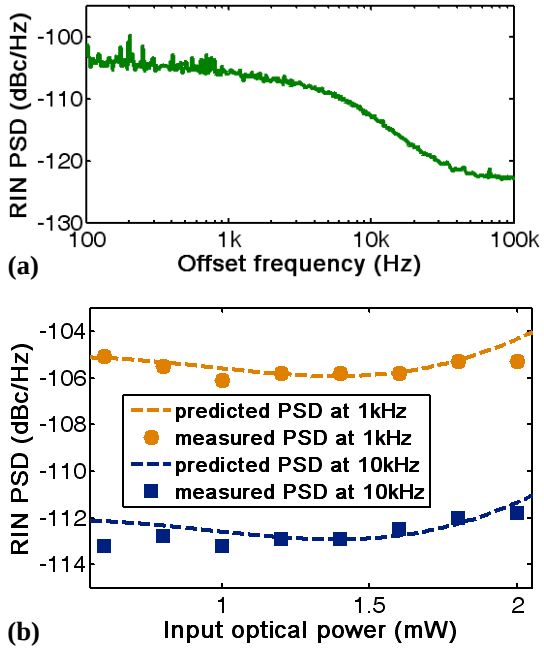

Fig.4. (a) Laser RIN power spectral density and (b) the PSD values at 1 kHz and 10 kHz offset frequencies (circle and square markers) compared with the predicted values (dashed lines) with different input optical powers.

IV. Effect of Pulse Width and Peak Power of the Incident Optical Pulses

Previous research has shown that the impulse response of the PDs is also affected by the peak power (and thereby the pulse width) for a given average power of the incident optical pulses [30]. We now investigate this effect in the context of small pulse width by inserting a certain length of single mode fiber (SMF) between the VOA and the PD in Fig. 1. The pigtails of the VOA are 2 m SMF. Four different SMF lengths 2 m, 4 m, 12 m and 22 m are considered and the measurements are carried out at 1.8 mW input power. These fiber lengths result in increased optical pulse widths of 0.7 ps, 1 ps, 2.1 ps, 3.6 ps, respectively, and a corresponding decrease in the incident peak power. The pulse widths are quite insensitive to the input power

injected into the SMF. A decrease of input power from 1.8mW to 0.2mW leads to a less than 10% increase of pulse widths. Fig.7 gives an example of measured pulse profiles at two input power levels of 0.4 mW and 1.4 mW for different SMF lengths (VOA is used to compensate the different values of the insertion loss of the SMF and fiber connectors). It can be seen that the optical pulses with a wider pulse width (and lower peak power) typically generate electrical pulses with lower amplitudes and narrower pulse widths; this in turn leads to a change in the noise conversion ratios. Fig.8 shows the calculated noise conversion ratios r_{PWJ}, r_{RAN_P} and r_{RAN_R} with a 4 m SMF which confirms the validity of Eq.(15). Fig.9 summarizes the ratios r_{PWJ} and r_{RAN_R} for all four different lengths of SMF. Compared with the ratios measured with 2 m SMF, the change is less than 0.15 in both r_{PWJ} and r_{RAN_R}, indicating that the effect of changing incident optical pulse width and peak power is very limited on r_{PWJ} , r_{RAN_P} and r_{RAN_R}.

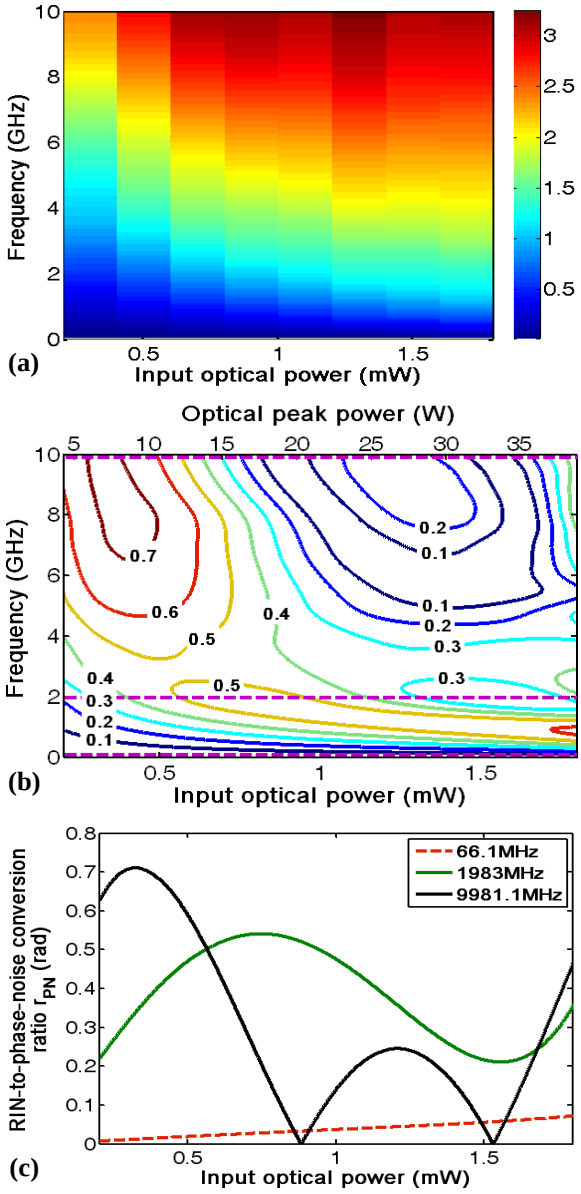

Fig.5. (a) Phase values in radians as a function of frequency and average input optical power levels (b) RIN-to-phase-noise conversion ratio r_{PN} in radians after the fourth-order polynomial fit of the phases in (a). Note the different optical peak powers corresponding to different input optical powers. (c) Three examples of the RIN-to-phase-noise conversion ratios corresponding to the three dashed lines in (b)

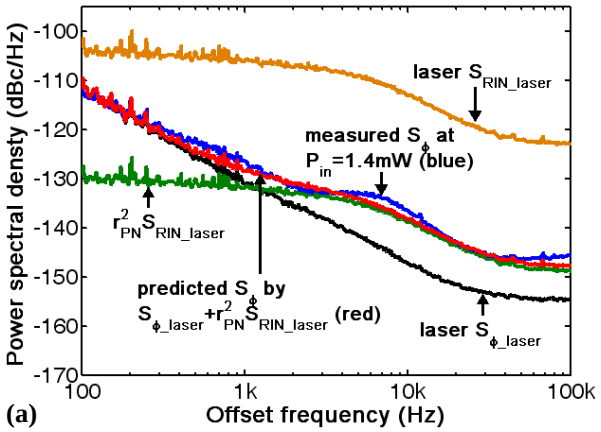

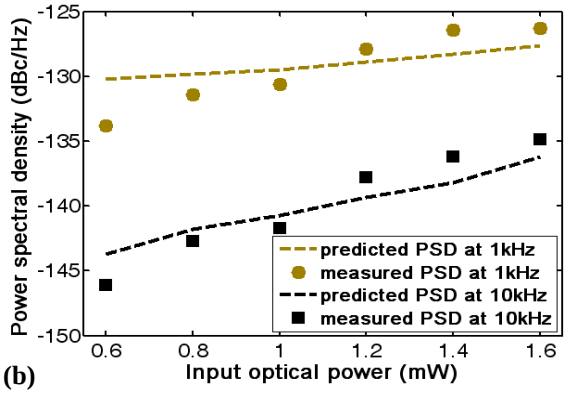

Fig.6. (a) Phase noise PSD prediction at an input power of 1.4 mW. (b) Predicted and measured phase noise PSD values at 1 kHz and 10 kHz offset frequencies under different input optical power.

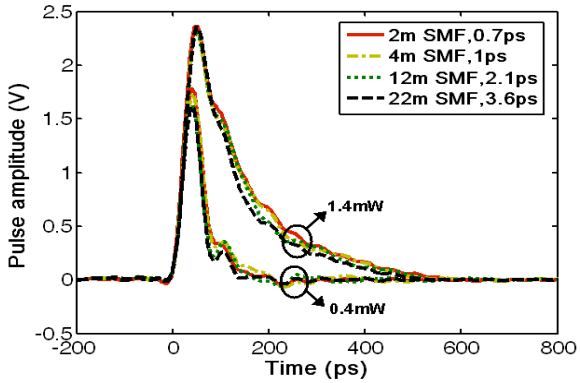

Fig.7. Electrical pulse profiles measured at two input optical power levels of 0.4 mW and 1.4 mW for different SMF lengths and pulse widths.

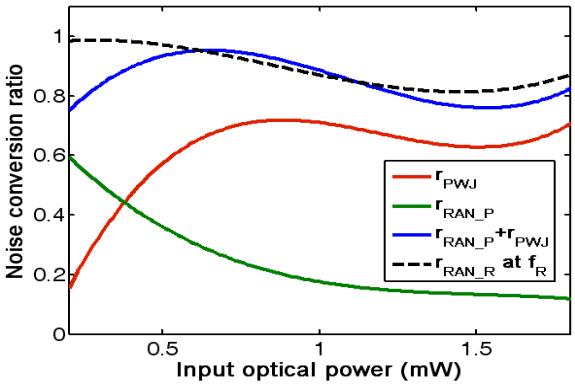

Fig.8. Noise conversion ratios with 4 m SMF (1 ps pulse width)

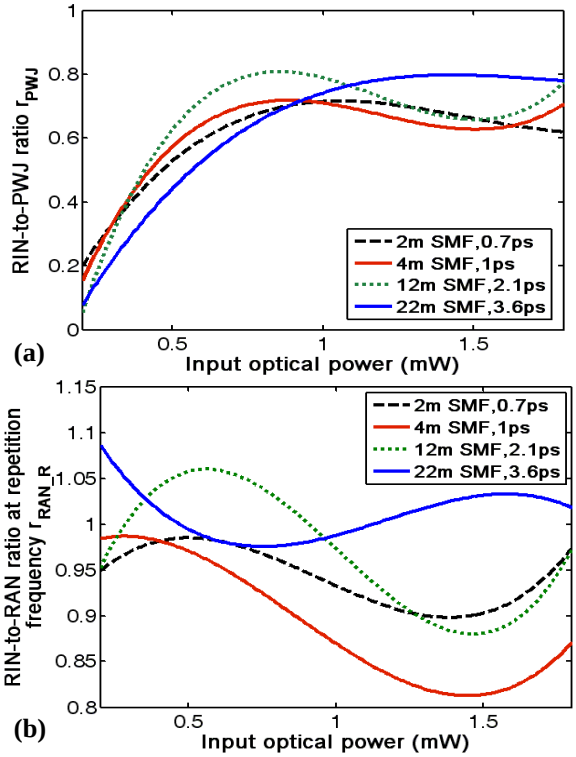

Fig.9. (a) RIN-to-PWJ conversion ratio r_{PWJ} (b) RIN-to-RAN (RAN at f_R) conversion ratio r_{RAN_R} for different SMF lengths and pulse widths.

The RIN-to-phase-noise conversion ratio values measured for different SMF lengths are also considered and shown in Fig.10. It can be seen that a change in the incident optical pulse width (and peak power) leads to a change of r_{PN} especially when the frequency is higher than 2 GHz. This suggests that the optical-pulse-width-dependent (or peak-power-dependent) impulse response of the PD is mainly due to the response at high frequency components. Also, it seems to be more convenient to use incident optical pulse width rather than the previously used optical peak power to describe this effect because the pulse width is quite insensitive to the input power injected into the SMF before PD due to the weak fiber nonlinear effect whereas peak power is directly affected both by the input power and pulse width. This means the pulse width and input power can be treated as two independent and "orthogonal" variables which can be controlled individually for actual microwave signal synthesis application. For the 10 GHz PD, it is found that the ratios r_{PN} in Fig.10 (b) and (c) are nearly identical which indicates that an increase in optical pulse width beyond 2.1 ps (corresponding to 12 m SMF) has very limited effect on the RIN-to-phase-noise conversion ratios for a given frequency and input optical power.

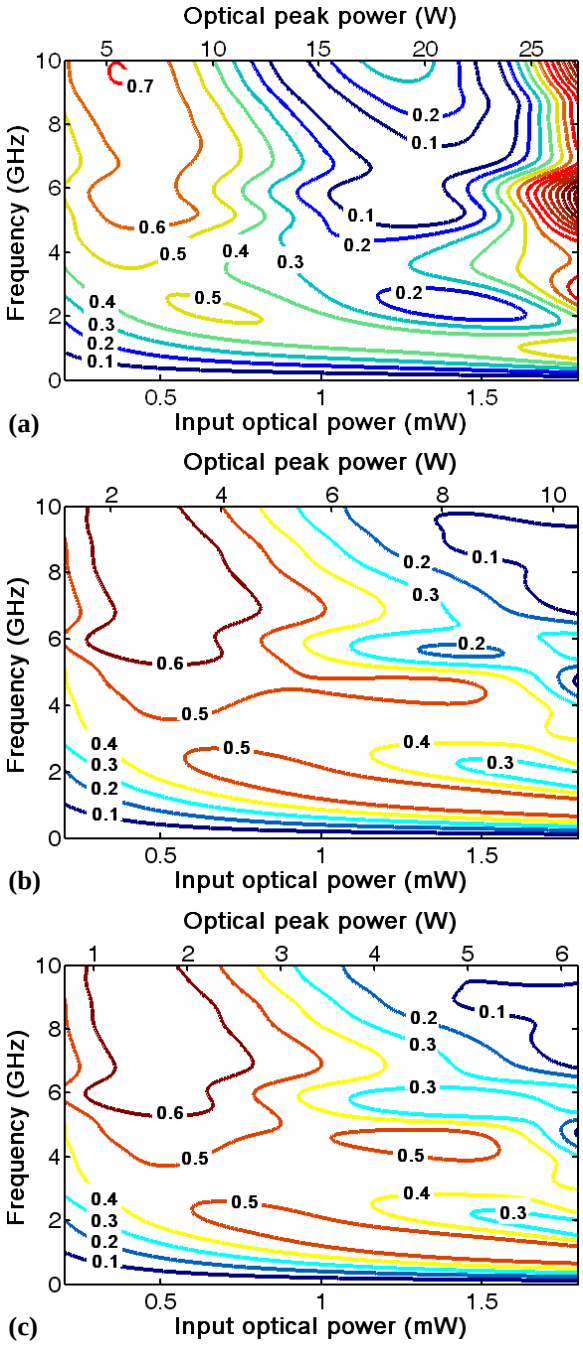

Fig.10. RIN-to-phase-noise conversion ratios r_{PN} (in radians) for different SMF lengths (a) 4 m (1 ps pulse width), (b) 12 m (2.1 ps pulse width) and (c) 22 m (3.6 ps pulse width) for the 10 GHz PD. Note the different optical peak power levels corresponding to average input optical power levels for each SMF length.

For low-noise microwave signal synthesis applications, a proper operating point of the PDs should be chosen to achieve low RIN-to-phase-noise conversion. For example, if we use the 10 GHz PD to generate a signal at 10 GHz and define an acceptable range of r_{PN} as 0~0.1 (corresponding to a maximum

RIN-to-phase-noise conversion ratio of -20 dB in PSD), the corresponding acceptable input power ranges according to Fig.5 (b) and Fig.10 are 0.82-0.96 mW & 1.45-1.60 mW for 2 m SMF (0.7 ps optical pulse width) and 0.84-0.96 mW & 1.48-1.56 mW for 4 m SMF lengths (1 ps optical pulse width) and none for the remaining two SMF lengths. It is worth mentioning that a wider optical pulse width (or a lower peak power) does not necessarily lead to a lower r_{PN} and a wider acceptable input power range. One can see that for 10 GHz frequency, acceptable input power ranges are wider for narrower optical pulse widths; on the other hand the input power range can also be wider for wider optical pulse widths at other frequencies, e.g., 9 GHz.

V. Effect of the Saturation Power of Photodetectors

In many applications of low-noise microwave signal synthesis, a wideband PD is used. This may implicitly suggest that a wideband PD should have a low RIN-to-phase-noise conversion. However, our comparison of two PDs with 10 GHz and 2 GHz bandwidth respectively, shows that this is not necessarily true and the saturation power of the PDs may play an even more important role to achieve low RIN-to-phase-noise conversion. We show in Fig.11 the measured impulse response of a 2 GHz PD (Thorlabs DET01CFC) for various input optical powers. The experimental conditions are exactly the same as those for the 10 GHz PD covered in section III. RIN-to-phase-noise conversion ratio r_{PN} is shown in Fig.12 (a). For comparison, we re-plot the r_{PN} contours of the 10 GHz PD for frequencies below 2 GHz in Fig.12 (b).

It is seen that for the 2 GHz PD when the input power is below ~0.5 mW, only the amplitude of the output pulses increases linearly with increasing optical input power and the pulse width and pulse profile are nearly unchanged. This means that the pulse "gravity center" is nearly unchanged and thus the excess phase noise converted from the optical intensity noise is low. When the input power is higher than 0.5 mW, the pulse distortion of the 2 GHz PD becomes significant, leading to a quick increase of r_{PN}. On the contrary, for the 10 GHz PD, both the amplitude and pulse width of the output pulses increase with the input power for input powers starting as low as ~0.2 mW (see Fig.3 (a)) and thus the pulse "gravity center" is changed accordingly, leading to a higher phase noise conversion ratio r_{PN}.

We can define an impulse-response saturation power (IRSP) below which increasing input optical power leads to a linear increase of electrical pulse amplitude with pulse width and pulse profile nearly unchanged. The IRSP is ~0.5 mW for the 2 GHz PD and ~0.2 mW for the 10 GHz PD. Our experimental observation suggests that the RIN-to-phase-noise conversion is low when the input power is below the IRSP although r_{PN} may not be necessarily less than 0.1 for some frequencies (see Fig.12). The PD with a higher IRSP is preferred to allow a wider acceptable input power range (assuming that it has a sufficient bandwidth for the application) while maintaining a low excess phase noise $r_{PN} < 0.1$. This is also supported by the experimental observations on the PDs with similar bandwidth but different IRSP reported in [22].

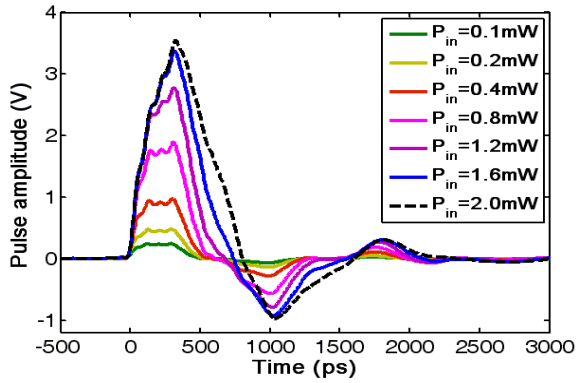

Fig.11. Electrical pulse profiles for different input optical powers incident on a 2 GHz PD.

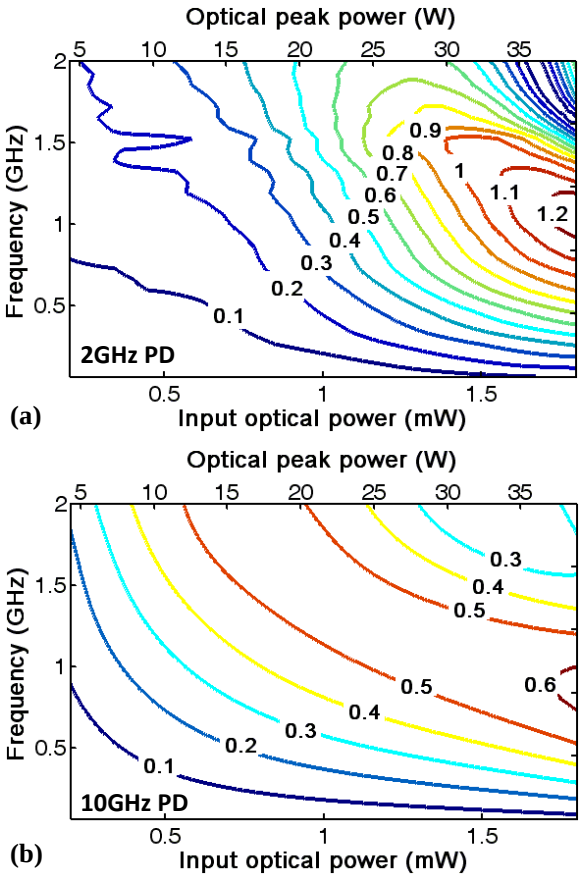

Fig.12. RIN-to-phase-noise conversion ratios r_{PN} (in radians) of (a) 2 GHz PD and (b) 10 GHz PD.

Another observation is that, at a given input power, a PD with narrower bandwidth concentrates the power to a few low frequency components whereas a PD with wider bandwidth distributes the power averagely to a wide range of frequency components. Therefore, the lower frequency components of a PD with narrow bandwidth have higher power than those of a PD with wide bandwidth. This suggests that a PD with just the necessary bandwidth is meaningful for real applications of microwave signal synthesis because higher output power can suppress shot and thermal noise, e.g., to generate a 1 GHz signal a PD with a bandwidth of 2 GHz can provide higher power at 1 GHz than a PD with a bandwidth of 10 GHz.

VI. Conclusion

In conclusion, we have presented a method for the detailed characterization of the excess noise conversion from optical RIN to electrical pulse width jitter, relative amplitude noise and phase noise in the photodetectors when detecting the optical pulse train from mode-locked lasers. It has been shown that the RIN-to-PWJ, RIN-to-RAN (RAN of pulse amplitude) and RIN-to-phase- noise conversion ratios can be obtained by analyzing the electrical pulse profiles measured by a high-speed oscilloscope for different input optical powers. The RIN-to-RAN (RAN at f_R) has been obtained by measuring the power at the repetition frequency by an RF spectrum analyzer for different input optical powers. Theoretical analysis has been presented to describe the relations among these noise conversion ratios and to predict the measured electrical RAN and phase noise power spectral densities. Also, optical pulses with the same average power but different pulse width and peak power are found to affect the noise conversion ratios of the PDs due to their optical-pulse-width-dependent impulse response, especially for the RIN-to-phase-noise conversion ratio at high frequencies. This method can be applied to any kind of PDs for noise characterization; however the exact noise conversion ratios for a certain PD are dependent on its design. A PD with higher impulse-response saturation power is found to allow a larger input optical power range in which the RIN-to-phase-noise conversion ratio is less than 0.1. These results provide many useful guidelines for achieving low-noise photodetection in microwave signal synthesis application: a PD with higher impulse-response saturation power allows a wider range of input power levels while maintaining the excess phase noise to a low value. In addition, a proper operating point of the PD with respect to the input optical power and the optical pulse width needs to be chosen to obtain a low value of excess phase noise.

Appendix

The coefficient a_k of $\sum_{n=-\infty}^{+\infty} f_e(\frac{t-nT}{\tau})$ is defined in Eq.(26) where normalized time $x=t/\tau$ and duty cycle $\sigma=\tau/T$.

$$\begin{aligned} a_k &\equiv \frac{2}{T}\int_{-T/2}^{T/2} f_e(\frac{t}{\tau})\cos k\omega_R t dt \\ &= 2\sigma\int_{-1/2\sigma}^{1/2\sigma} f_e(x)\cos(2\pi kx\sigma)dx \end{aligned} \tag{26}$$

The coefficient c_k of $\sum_{n=-\infty}^{+\infty} \dot{f}_e(\frac{t-nT}{\tau})\frac{t-nT}{\tau}$ is defined in Eq.(27) and Eq. (28) where we assume the pulse width is much smaller than the period and thus $f_e(1/2\sigma)=0$. Also note that $c_0=0$.

$$\begin{aligned} c_k - a_k &\equiv \frac{2}{T}\int_{-T/2}^{T/2} \dot{f}_e(\frac{t}{\tau})\frac{t}{\tau}\cos k\omega_R t dt \\ &= 2\sigma\int_{-1/2\sigma}^{1/2\sigma} \dot{f}_e(x)x\cos(2\pi kx\sigma)dx \\ &= 2f_e(1/2\sigma)(-1)^k + 2\sigma\int_{-1/2\sigma}^{1/2\sigma} f_e(x)2\pi kx\sigma\sin(2\pi kx\sigma)dx \\ &\quad - 2\sigma\int_{-1/2\sigma}^{1/2\sigma} f_e(x)\cos(2\pi kx\sigma)dx \end{aligned} \tag{27}$$

$$c_k = 2\sigma\int_{-1/2\sigma}^{1/2\sigma} f_e(x)2\pi kx\sigma\sin(2\pi kx\sigma)dx \tag{28}$$

The coefficient b_k of $\sum_{n=-\infty}^{+\infty} f_o(\frac{t-nT}{\tau})$ is defined in Eq.(29).

$$\begin{aligned} b_k &\equiv \frac{2}{T}\int_{-T/2}^{T/2} f_o(\frac{t}{\tau})\sin k\omega_R t dt \\ &= 2\sigma\int_{-1/2\sigma}^{1/2\sigma} f_o(x)\sin(2\pi kx\sigma)dx \end{aligned} \tag{29}$$

The coefficient d_k of $\sum_{n=-\infty}^{+\infty} \dot{f}_o(\frac{t-nT}{\tau})\frac{t-nT}{\tau}$ is defined in Eq.(30) and Eq.(31)

$$\begin{aligned} d_k - b_k &\equiv \frac{2}{T}\int_{-T/2}^{T/2} \dot{f}_o(\frac{t}{\tau})\frac{t}{\tau}\sin k\omega_R t dt \\ &= 2\sigma\int_{-1/2\sigma}^{1/2\sigma} \dot{f}_o(x)x\sin(2\pi kx\sigma)dx \\ &= -2\sigma\int_{-1/2\sigma}^{1/2\sigma} f_o(x)2\pi kx\sigma\cos(2\pi kx\sigma)dx \\ &\quad - 2\sigma\int_{-1/2\sigma}^{1/2\sigma} f_o(x)\sin(2\pi kx\sigma)dx \end{aligned} \tag{30}$$

$$d_k = -2\sigma\int_{-1/2\sigma}^{1/2\sigma} f_o(x)2\pi kx\sigma\cos(2\pi kx\sigma)dx \tag{31}$$

References

[1] G. C. Valley, "Photonic analog-to-digital converters," *Opt. Express*, vol. 15, pp. 1955-1982, 2007.

[2] E. N. Ivanov, S. A. Diddams, and L. Hollberg, "Study of the excess noise associated with demodulation of ultra-short infrared pulses," *Ultrasonics, Ferroelectrics and Frequency Control, IEEE Transactions on*, vol. 52, pp. 1068-1074, 2005.

[3] J. Kim, J. A. Cox, J. Chen, and F. X. Kartner, "Drift-free femtosecond timing synchronization of remote optical and microwave sources," *Nat Photon*, vol. 2, pp. 733-736, 2008.

[4] S. M. Foreman, K. W. Holman, D. D. Hudson, D. J. Jones, and J. Ye, "Remote transfer of ultrastable frequency references via fiber networks," *Review of Scientific Instruments*, vol. 78, pp. 021101-25, 2007.

[5] H. A. Haus and A. Mecozzi, "Noise of mode-locked lasers," *Quantum Electronics, IEEE Journal of*, vol. 29, pp. 983-996, 1993.

[6] D. v. d. Linde, "Characterization of the Noise in Continuously Operating Mode-Locked Lasers," *Appl. Phys. B*, vol. 39, pp. 201-217, 1986.

[7] S. Namiki and H. A. Haus, "Noise of the stretched pulse fiber laser. I. Theory," *Quantum Electronics, IEEE Journal of*, vol. 33, pp. 649-659, 1997.

[8] R. Paschotta, "Noise of mode-locked lasers (Part I): numerical model," *Appl. Phys. B*, vol. 79, pp. 153-162, 2004.

[9] R. Paschotta, "Noise of mode-locked lasers (Part II): timing jitter and other fluctuations," *Appl. Phys. B*, vol. 79, pp. 163-173, 2004.

[10] R. Paschotta, "Timing jitter and phase noise of mode-locked fiber lasers," *Opt. Express*, vol. 18, pp. 5041-5054, 2010.

[11] S. Gee, F. Quinlan, S. Ozharar, P. J. Delfyett, J. J. Plant, and P. W. Juodawlkis, "Ultralow-noise mode-locked optical pulse trains from an external cavity laser based on a slab coupled optical waveguide amplifier (SCOWA)," *Opt. Lett.*, vol. 30, pp. 2742-2744, 2005.

[12] O. Prochnow, R. Paschotta, E. Benkler, U. Morgner, J. Neumann, D. Wandt, and D. Kracht, "Quantum-limited noise performance of a femtosecond all-fiber ytterbium laser," *Opt. Express*, vol. 17, pp. 15525-15533, 2009.

[13] K. Wu, J. H. Wong, P. Shum, D. R. C. S. Lim, V. K. H. Wong, K. E. K. Lee, J. Chen, and E. D. Obraztsova, "Timing-jitter reduction of passively mode-locked fiber laser with a carbon nanotube saturable absorber by optimization of cavity loss," *Opt. Lett.*, vol. 35, pp. 1085-1087, 2010.

[14] C. Ouyang, P. Shum, H. Wang, J. Haur Wong, K. Wu, S. Fu, R. Li, E. J. R. Kelleher, A. I. Chernov, and E. D. Obraztsova, "Observation of timing jitter reduction induced by spectral filtering in a fiber laser mode locked with a carbon nanotube-based saturable absorber," *Opt. Lett.*, vol. 35, pp. 2320-2322, 2010.

[15] Y. Song, K. Jung, and J. Kim, "Impact of pulse dynamics on timing jitter

in mode-locked fiber lasers," *Opt. Lett.*, vol. 36, pp. 1761-1763, 2011.
[16] L. Nugent-Glandorf, T. A. Johnson, Y. Kobayashi, and S. A. Diddams, "Impact of dispersion on amplitude and frequency noise in a Yb-fiber laser comb," *Opt. Lett.*, vol. 36, pp. 1578-1580, 2011.
[17] E. N. Ivanov, J. J. McFerran, S. A. Diddams, and L. Hollberg, "Noise properties of microwave signals synthesized with femtosecond lasers," *Ultrasonics, Ferroelectrics and Frequency Control, IEEE Transactions on*, vol. 54, pp. 736-745, 2007.
[18] R. P. Scott, C. Langrock, and B. H. Kolner, "High-dynamic-range laser amplitude and phase noise measurement techniques," *Selected Topics in Quantum Electronics, IEEE Journal of*, vol. 7, pp. 641-655, 2001.
[19] K. Wu, J. H. Wong, P. Shum, S. Fu, C. Ouyang, H. Wang, E. J. R. Kelleher, A. I. Chernov, E. D. Obraztsova, and J. Chen, "Nonlinear coupling of relative intensity noise from pump to a fiber ring laser mode-locked with carbon nanotubes," *Opt. Express*, vol. 18, pp. 16663-16670, 2010.
[20] J. Kim, J. Chen, J. Cox, and F. X. Kärtner, "Attosecond-resolution timing jitter characterization of free-running mode-locked lasers," *Opt. Lett.*, vol. 32, pp. 3519-3521, 2007.
[21] J. A. Cox, A. H. Nejadmalayeri, J. Kim, and F. X. Kärtner, "Complete characterization of quantum-limited timing jitter in passively mode-locked fiber lasers," *Opt. Lett.*, vol. 35, pp. 3522-3524, 2010.
[22] J. Taylor, S. Datta, A. Hati, C. Nelson, F. Quinlan, A. Joshi, and S. Diddams, "Characterization of Power-to-Phase Conversion in High-Speed P-I-N Photodiodes," *Photonics Journal, IEEE*, vol. 3, pp. 140-151, 2011.
[23] K. Wu, C. Ouyang, J. H. Wong, S. Aditya, and P. Shum, "Frequency Response of the Noise Conversion From Relative Intensity Noise to Phase Noise in the Photodetection of an Optical Pulse Train," *Photonics Technology Letters, IEEE*, vol. 23, pp. 468-470, 2011.
[24] J. Millo, R. Boudot, M. Lours, P. Y. Bourgeois, A. N. Luiten, Y. L. Coq, Y. Kersalé, and G. Santarelli, "Ultra-low-noise microwave extraction from fiber-based optical frequency comb," *Opt. Lett.*, vol. 34, pp. 3707-3709, 2009.
[25] J. Kim and F. X. Kärtner, "Microwave signal extraction from femtosecond mode-locked lasers with attosecond relative timing drift," *Opt. Lett.*, vol. 35, pp. 2022-2024, 2010.
[26] K. J. Granta, H.-F. Liub, and R. Janb, "Spectral technique for measuring the pulse-width jitter of a gain-switched laser," *Optics Communications*, vol. 213, pp. 183-186, 2002.
[27] O. Pottiez, O. Deparis, R. Kiyan, P. Mégret, and M. Blondel, "Measurement of pulse width and amplitude jitter noises of gigahertz optical pulse trains by time-domain demodulation," *Opt. Lett.*, vol. 26, pp. 1779-1781, 2001.
[28] I. G. Fuss, "An interpretation of the spectral measurement of optical pulse train noise," *Quantum Electronics, IEEE Journal of*, vol. 30, pp. 2707-2710, 1994.
[29] L. P. Chen, Y. Wang, and J. M. Liu, "Spectral measurement of the noise in continuous-wave mode-locked laser pulses," *Quantum Electronics, IEEE Journal of*, vol. 32, pp. 1817-1825, 1996.
[30] P.-L. Liu, K. J. Williams, M. Y. Frankel, and R. D. Esman, "Saturation characteristics of fast photodetectors," *Microwave Theory and Techniques, IEEE Transactions on*, vol. 47, pp. 1297-1303, 1999.

Kan Wu (S'09) received the B.S. and M.S. degree in electronic engineering from Shanghai Jiao Tong University in 2006 and 2009, respectively.

He is currently pursuing the Ph.D. degree in electrical and electronic engineering in Nanyang Technological University, Singapore. His research interests include low-noise mode-locked lasers, pulse train noise measurement and carbon nanotubes based devices.

Ping Shum (S'93-M'95-SM'05) received the B. Eng. and PhD degrees in electronic and electrical engineering from the University of Birmingham, UK, in 1991 and 1995, respectively.

In 1996, he joined the Hong Kong University. Since July 1997, he joined the City University of Hong Kong. In 1999, he joined the School of Electrical and Electronic Engineering, Nanyang Technological University. He was the founding member of IEEE Photonics Society Singapore Chapter. Since 2002, he has been appointed as the Director of Network Technology Research Centre. He received the Singapore National Academy of Science Young Scientist Award in 2002 for his contributions on optical communication technology. Dr. Shum has published more than 300 papers. He was the chair, committee member and international advisor of many international conferences (e.g. ICOCN, OECC, ECOC, COIN, ACP, ICMAT, ICICS and Photonics Global). His research interests are concerned with optical communications, nonlinear waveguide modeling, fiber gratings and WDM communication systems.

Sheel Aditya (S'76-M'80-SM'94) received his B.Tech. and Ph.D. in Electrical Engineering from IIT Delhi in 1974 and 1979, respectively. From 1979-2001, he held academic positions ranging from lecturer to professor in the Electrical Engineering Department, IIT Delhi. Since 2001, he is an Associate Professor in the School of Electrical and Electronic Engineering, Nanyang Technological University, Singapore. Dr. Aditya has research interests in planar microwave waveguides and antennas, microwave photonics, and optical fiber communication. He has been involved in a number of research & development projects and jointly holds three patents in India and Singapore. He has held visiting assignments at Chalmers University of Technology, Sweden, Indian Institute of Science, Bangalore, India, Florida State University, USA, and Nanyang Technological University, Singapore. Dr. Aditya is a Senior Member of IEEE and Fellow of IETE (India) since 1994.

Chunmei Ouyang received the M.S. degree in optical engineering from Harbin Engineering University, Harbin, China, in 2006. She received the Ph. D degree in optical electronic technology from Tianjin University, Tianjin, China. She is currently working as a Postdoctoral Fellow in Nanyang Technological University, Singapore.

Her research is focused on high power passively mode-locked fiber lasers and low timing jitter mode-locked fiber lasers.

Jia Haur Wong (S'09) received the B.A. degrees in Electrical and Electronic Engineering from Nanyang technological University at Singapore in 2009. He is currently pursuing the Ph.D degree in Electrical and Electronic Engineering at Nanyang technological University at Singapore. His current research is in the area of low noise fiber laser and microwave photonics systems.

Huy Quoc Lam received the BE in electrical and electronics engineering from Ho Chi Minh City University of Technology, Vietnam in 1999, the Master of Telecommunications Engineering from Monash University, Australia in 2005, and PhD from Nanyang Technological University, Singapore in 2009. He is now a research scientist at the Nanyang Technological University.

His research interests include fiber lasers, optical signal processing, photonic analog-to-digital conversion and nonlinear optics.

Kenneth E. Lee received the B.S. and M.S. degrees from the University of Illinois at Urbana-Champaign in 1998 and 1999, respectively, and the Ph.D. degree from the Massachusetts Institute of Technology in 2009, all in Electrical Engineering. Since 2001, he has been with the Applied Physics Laboratory in DSO National Laboratories, Singapore, where he is Senior Member of Technical Staff. He has worked on various projects in the fields of microwave photonics, semiconductor lasers and solid-state lasers. In 2009, he assumed an adjunct position at Temasek Laboratories at Nanyang Technological University, Singapore, where he currently manages the Photonics Program.

He is currently investigating novel microwave photonic systems and components, and studying the development of various optoelectronic devices using both III-As/P MOCVD and III-N MBE.